

## Article

# Aging Study of Plastics to Be Used as Radiative Cooling Wind-Shields for Night-Time Radiative Cooling—Polypropylene as an Alternative to Polyethylene

Ingrid Martorell <sup>\*</sup>, Jaume Camarasa, Roger Vilà , Cristian Solé and Albert Castell 

Sustainable Energy, Machinery and Buildings (SEMB) Research Group, INSPIRES Research Centre, Universitat de Lleida, Pere de Cabrera s/n, 25001 Lleida, Spain

<sup>\*</sup> Correspondence: ingrid.martorell@udl.cat

**Abstract:** Polyethylene has widely been used in radiative cooling applications because of high transmittance values in the atmospheric window. However, it presents optical and mechanical degradation when exposed to environmental conditions and must be replaced every few months. This paper aims to find an alternative to polyethylene to be used in a unique device, the Radiative Collector and Emitter (RCE), that combines solar collection and night-time radiative cooling. The aging evolution analysis of five cheap and market available plastic films (two low density polyethylene, one high density polyethylene, one polypropylene, and one fluorinated ethylene propylene) exposed to environmental conditions was performed. FT-IR spectra and mechanical traction tests were performed before and after 90 days of exposure to the environment. Results confirm that polyethylene undergoes a degradation process both when it is covered by a glass and when it is uncovered. However, it maintains high average transmittance values in the atmospheric window. Polypropylene has average transmittance values slightly lower than polyethylene, but its aging behaviour is better since no oxidative processes are detected when the material is covered with glass. For all this, PP-35 is an interesting candidate for night-time radiative cooling wind-shields.

**Keywords:** night-time radiative cooling; wind-shield; plastic films; transmittance; mechanical tests; aging



**Citation:** Martorell, I.; Camarasa, J.; Vilà, R.; Solé, C.; Castell, A. Aging Study of Plastics to Be Used as Radiative Cooling Wind-Shields for Night-Time Radiative Cooling—Polypropylene as an Alternative to Polyethylene. *Energies* **2022**, *15*, 8340. <https://doi.org/10.3390/en15228340>

Academic Editor: Kian Jon Chua

Received: 30 September 2022

Accepted: 3 November 2022

Published: 8 November 2022

**Publisher's Note:** MDPI stays neutral with regard to jurisdictional claims in published maps and institutional affiliations.



**Copyright:** © 2022 by the authors. Licensee MDPI, Basel, Switzerland. This article is an open access article distributed under the terms and conditions of the Creative Commons Attribution (CC BY) license (<https://creativecommons.org/licenses/by/4.0/>).

## 1. Introduction

Energy consumption has been increasing worldwide due to modern society energy demands. In the European Union, 40% of the total energy consumption is in buildings. The Eurostat [1] concludes that space heating represents 64.1% of the total consumption in buildings, domestic hot water (DHW) 14.8%, and space cooling 0.3%. A recent report by the International Energy Agency predicts also that refrigeration demands will triple worldwide by 2050 if no action is taken [2]. Thus, there is a need for covering heating and cooling energy demands by using more efficient systems.

Solar thermal collectors are a mature and commercially implemented technology to produce hot water from renewable energy. Highly efficient solar collectors for exploiting solar irradiation in an optimum way have been developed in the last decades [3]. Most current cooling systems run on compression cooling cycles, consuming high amounts of electricity, especially in the summer heat peaks. An alternative to produce cold is solar cooling, combining solar thermal collectors with an absorption heat pump. Absorption heat pumps reduce the electrical energy consumption but presents drawbacks such as low efficiency, the lack of small capacity units, and the need of high temperatures (>100 °C) to increase their efficiency [4]. Moreover, auxiliary equipment is required, such as the absorption chiller and the cooling tower, which increases the cost of the installation and can result in health problems such as *Legionella*. Another renewable alternative to produce cold is radiative cooling.

Radiative cooling [5] is a phenomenon that has its origins in a physical principle discovered by the German mathematician and physicist Max Planck and it is based on the simple fact that all bodies radiate energy to the outside at a specific wavelength. This radiation depends on the body temperature and the low effective temperature of the space makes it possible to cool down below ambient temperature [6,7]. Therefore, when a body is at higher temperature than the space, energy is radiated to the space and, consequently, the body cools down. This cooling should be considered a renewable cooling, in the sense that no additional energy input is needed to induce this cooling to happen. In other words, heat transfer by cooling radiation occurs continuously and spontaneously in a spectral region of wavelengths, specifically at long-bandwidths between 7 and 14  $\mu\text{m}$  (located in the so-called infrared region, and commonly known as the atmospheric window) where the atmosphere has a relatively low absorption. Since the atmosphere is mostly transparent at these wavelengths and does not absorb the energy emitted in this range, materials that emit radiation in the range of 7 to 14  $\mu\text{m}$  send it directly into space.

Combining both traditional solar collection during the day and cooling production during night-time, using exclusively renewable energy, has been proposed by several authors [8–12]. Vall et al. [10] presented for the first time a single device called a radiative collector and emitter (RCE), which combines solar heating and radiative cooling functionalities using an adaptive cover. Optical characteristics of this adaptive cover are different (almost opposite) for solar collection than for radiative cooling. While the solar collection requires a cover with high transmittance of radiation in 0.2–4  $\mu\text{m}$  wavelengths and a low transmittance for the rest of wavelengths, the radiative cooling surface requires a high transmittance in the wavelength range between 7–14  $\mu\text{m}$  (to radiate to the outer space through the atmospheric window). Moreover, the absorber/emitter surface used for both heating and cooling purposes should have a high absorptivity/emissivity in the full solar and infrared (IR) spectrum (broad-band emitter), in contrast to the selective or narrow-band surfaces used in conventional solar collectors and radiative coolers [13,14]. More recently, other researchers have also proposed this idea of producing both heating and cooling, but with other solutions [15,16], especially using spectrally selective materials used as radiative cooler emitters. Other studies focused on the combination of both strategies, selective covers, and emitters to achieve solar collection and night-time radiative cooling [17].

Solar collectors use a glass cover to act as a wind-shield, as it also provides a greenhouse effect. However, the use of glass is not compatible with radiative cooling, since it does not allow thermal radiation to pass through at the atmospheric infrared window, thus blocking radiative cooling. An adaptive cover is needed when hot water is produced during daytime (solar collector) and cold water is produced during night-time (radiative cooling). A traditional solar collector is modified to include a plastic film below the solar collector glass. This plastic film remains present in both modes (daytime solar collection and night-time radiative cooling). Several studies have demonstrated the importance of the use of a wind-shield for radiative cooling [18,19], in order to reduce the parasitic heat gains, and thus increase the cooling power. Although wind-shield materials for radiative cooling have been proposed, none of them fulfil all the requirements needed. Crystals, such as zinc crystals [20–22], are good candidates for having high resistance to environmental conditions, but their high price and the impossibility of manufacturing them in large dimensions make them unfeasible. Chromic materials [23,24] are promising materials for radiative cooling but fundamental research is still needed, and they are also expensive to produce. Plastics are basically the materials used in radiative cooling applications because they are cheap and can be produced in adequate dimensions. However, a drawback is that they have less resistance to external environmental conditions.

To date, films of polyethylene (PE) have been widely used as wind-shields for their high average transmittance values in the atmospheric window. Average transmittance values for 50  $\mu\text{m}$  low-density polyethylene (LDPE) films around 80% are found [25,26]. However, it is well known that polymers show degradation (thermal, oxidative, chemical, radiative and mechanical) when exposed to outdoor conditions. Abdelhafidi et al. [27]

reported that photodegradation of LDPE films is basically due to the ultraviolet (UV) radiation, which can be considered the most harmful factor of plastic degradation. Balocco et al. [28] also demonstrated that photooxidation of polyethylene plastic films implies a process of bonds breaking, increasing the amount of low molecular weight material, as well as an increase of its hydrophilicity by the presence of carbonyl groups. Plus, an embrittlement of the material is also detected [29]. Fourier transform infrared spectroscopy (FT-IR) and mechanical tests have been reported by different authors as suitable techniques to follow degradation of polymers [30–34]. Ali et al. [35] reported a substantial decrease of transmittance when exposing a 50  $\mu\text{m}$  polyethylene film to outdoor conditions for 100 days, which led to a reduction of the radiative cooling system cooling power by 33.3%. Martorell et al. [36] presented an experimental study where a decrease between 3.5% and 9% in the polyethylene average transmittances in the atmospheric window for three winter months of exposure to the environment was measured.

According to Zhang et al. [19] the wind-shield needs to have high mechanical strength to withstand outdoor weather conditions, such as strong winds, strong rain, and even hail. Mechanical tests such as traction tests give insight in this issue. Some authors [37–39] have focused research on finding the relationship between the change of the chemical structure and the change in mechanical properties. Carrasco et al. [30] show that the replacement of the C–H bonds for C=O bonds turns into an increase of the Young's modulus, producing a stiffness of the material.

Thus, it is important to find a material transparent to long-wave radiation (with high thermal transmittance in the wavelength range between 7–14  $\mu\text{m}$ ), highly resistant to abrasion and moisture, durable, with zero or very low degree of hygroscopicity, with a certain degree of hardness, certain tensile strength, and high degree of elasticity. As explained previously, polyethylene is widely used as a wind-shield for radiative cooling but it shows optical degradation when exposed outdoors and has poor mechanical performance. This work focuses on experimentally studying the optical and mechanical behavior of different high available and cheap plastic wind-shield candidates to find an alternative to polyethylene to be used as radiative cooling wind-shield for a solar collection and night-time radiative cooling applications.

## 2. Materials and Methods

The RCE prototype consists of a modified regular flat plate solar collector (2  $\text{m}^2$ ), with an adaptive cover to produce hot water during the day and cold water (below ambient temperature) at night (Figure 1).



**Figure 1.** (left) adaptive cover concept; (right) black surface as absorber/emitter, plastic film wind-shield for night-time radiative cooling, and glass for solar collection.

The adaptive cover (Figure 2) combines materials with different (almost opposite) optical properties for the solar collector and the radiative cooler. While the solar collection mode requires a cover with high transmittance of radiation in 0.2–4  $\mu\text{m}$  wavelengths and a low transmittance for the rest of wavelengths, the radiative cooling mode requires a high transmittance in the wavelength range between 7–14  $\mu\text{m}$  (to radiate to the outer space through the atmospheric window).

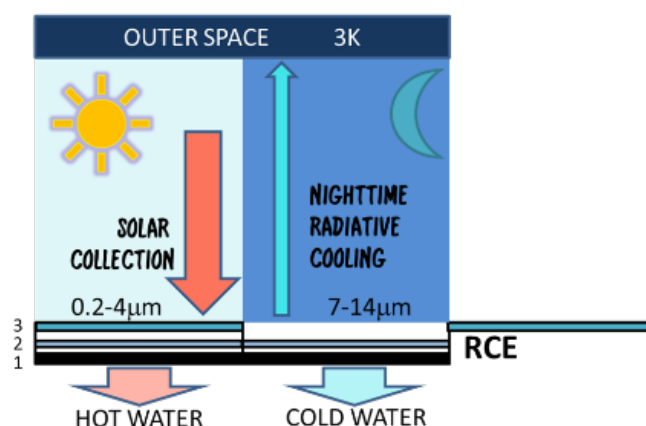


**Figure 2.** Radiative Collector and Emitter (RCE) working under solar collection mode (SC) during day time and radiative cooling mode during night-time. (1) absorber/emitter, (2) wind-shield (plastic film), and (3) glass cover.

### 2.1. Materials

Wind-shield candidates are presented in Table 1. All plastics chosen are visually transparent, highly available, and cheap. Two low density polyethylene samples of 100  $\mu\text{m}$  and 60  $\mu\text{m}$  (LPDE-100 and LPDE-60, respectively) were chosen with the objective of testing the thickness variable. Comparisons between LDPE-60 and high-density polyethylene (HDPE-60) were also studied. In addition, two widely used polymeric plastics, polypropylene (PP-35), and fluorinated ethylene propylene (FEP-50), were considered.

**Table 1.** Candidate materials for radiative cooling wind-shields.

Chemical Nomenclature	Thickness, $\mu\text{m}$	Nomenclature
Low-density polyethylene ( $\text{C}_2\text{H}_4$ ) <sub>n</sub>	96.3	LDPE-100
Low-density polyethylene ( $\text{C}_2\text{H}_4$ ) <sub>n</sub>	59	LDPE-60
High-density polyethylene ( $\text{C}_2\text{H}_4$ ) <sub>n</sub>	57.8	HDPE-60
Polypropylene ( $\text{C}_3\text{H}_6$ ) <sub>n</sub>	35.8	PP-35
Fluorinated ethylene propylene ( $\text{C}_2\text{F}_4$ ) <sub>n</sub>	50	FEP-50

Average thickness of the films was tested following UNE-ISO 4593:2010 by measuring 20 random equidistant samples per film with a micrometer (Heudenhain ND287, Traunreut, Germany) (Figure 3).



(a)



(b)

**Figure 3.** (a) 20 random samples in a LDPE film. (b) Heudenhain ND287 micrometer.

As an example, Figure 4 shows the thickness distribution for LDPE-100. Thickness differences along the plastic film were observed. The average tested thickness of this sample is 96.3  $\mu\text{m}$  with a micrometer error of  $\pm 0.5\%$ .

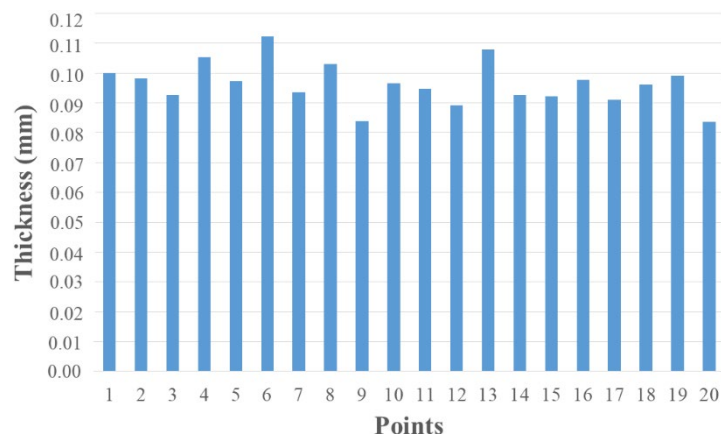


**Figure 4.** Thickness distribution for LDPE-100.

## 2.2. Experimental Setup

Plastic films were mounted in wood frames of  $13 \times 15 \text{ cm}^2$  each (Figure 5). The bottom of the frames was painted black. To study the influence of the glass present in the RCE solar collection mode, two experimental sets of frames were mounted in parallel, one without glass and the other with glass. Samples were cut in a longitudinal (L) or transversal (T) direction according to the extrusion process, as shown in Figure 5, and samples were extracted after 90 days. An experimental campaign of three months was performed because authors observed in a previous experimental campaign an average transmittance drop of 0.7% for 500  $\mu\text{m}$  PE exposed during two months in summer. According to this, the more significant transmissivity drop happens after the second month. In addition, Chabira et al. [32] show a dramatic drop after three months in both elongation at break and tensile strength for LDPE samples exposed 8 months to environmental conditions.

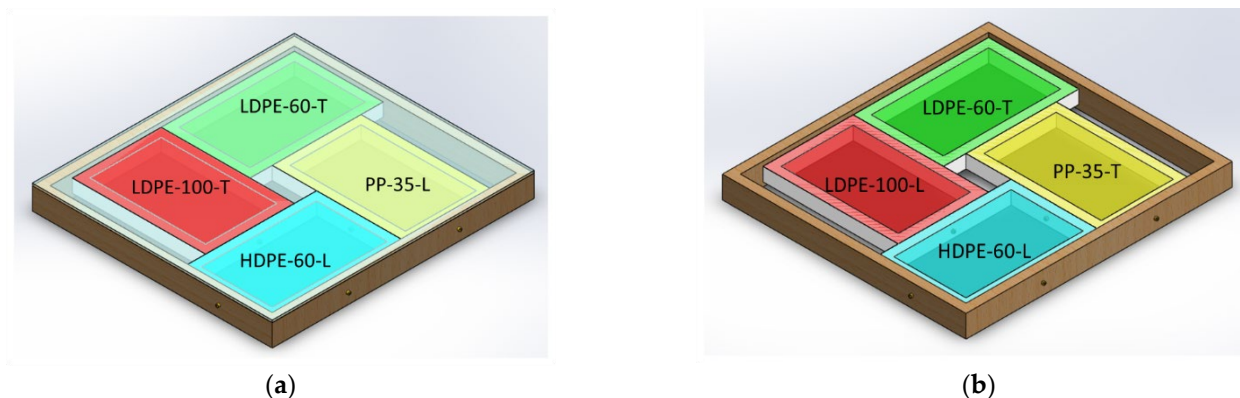


**Figure 5.** Experimental set up scheme. (a) Transparent films distribution with glass. (b) Transparent film distribution without glass.

The frames were located, avoiding shadows on the roof of the CREA Building at the University of Lleida (Catalonia, Spain), and the experimental campaign was performed from October 2020 to January 2021. Condensed water and accumulated dust were removed manually twice a week. During this period, plastics were exposed at maximum temperatures of 25  $^{\circ}\text{C}$  and minimum temperatures of 0  $^{\circ}\text{C}$ . Thus, a wide ambient temperature spectrum was covered during the experimental campaign.

### 2.3. Experimental Instruments and Sample Preparation

FT-IR spectra of plastic films were collected using a FT-IR spectrometer (Jasco FT-IR 6300 (Easton, MD, USA) with a diamond/ZnSe crystal) containing a DLATGS detector. The Jasco FT-IR 6300 counts with a wavenumber accuracy of  $\pm 0.01 \text{ cm}^{-1}$ , a resolution of  $4 \text{ cm}^{-1}$  and a sensitivity of  $S/N = 50,000:1$ . Each spectrum were recorded with 32 scans, in the 2500–15,384  $\text{nm}$  range (Figure 6).

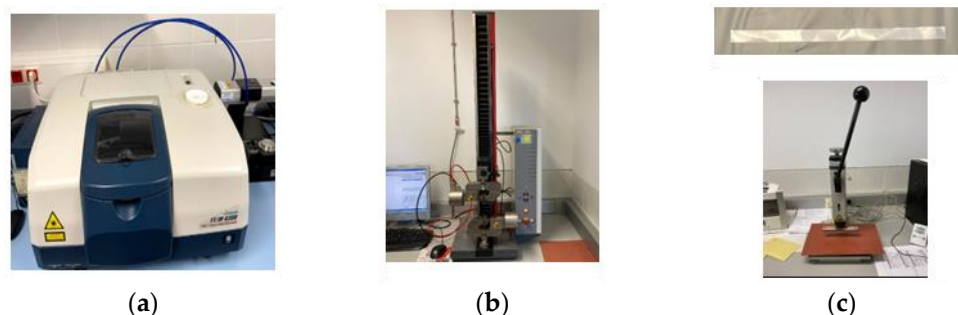


**Figure 6.** (a) Jasco FT-IR 6300; (b) ZwickRoell BZ1-MMZ2.5.ZW01; (c)  $1 \times 15 \text{ cm}$  specimen and press.

Three repetitions of each sample in Transmission mode were performed in the spectroscopy. Brand new samples with no environmental exposure (0 days) and samples after three months of exposure to the environment (90 days) were analyzed. Samples ( $6 \times 6 \text{ cm}$ ) to be analyzed by FT-IR were cut out from the plastic films and wiped with a dry cloth to remove accumulated dust. No other treatment was carried out.

Traction mechanical tests were performed in a ZwickRoell BZ1-MMZ2.5.ZW01 (Ulm, Germany) with a tolerance range of  $\pm 10\%$ , following ISO 527-1, ISO 527-2, and ISO 527-3. Five specimens of  $1 \times 15 \text{ cm}$  for each material were cut in a small press (Figure 6). Measurements were limited to the central part of the sample and each specimen was wiped dry to remove dust. Next, specimens were pinned to the jaw and force was exercised in the longitudinal or the transversal axis until the sample broke. Five repetitions of each specimen were conducted.

## 3. Results and Discussion

### 3.1. Optical Properties and Chemical Structure

Figure 7 shows FT-IR spectra for the five samples studied before being exposed to environmental conditions (0 days). No differences were observed in the three polyethylene samples analyzed, as expected. Polypropylene shows a lower transmittance than polyethylene samples and behaves different, with sharp absorption peaks. FEP sample is the one with lower transmittances values with wide absorption peaks.

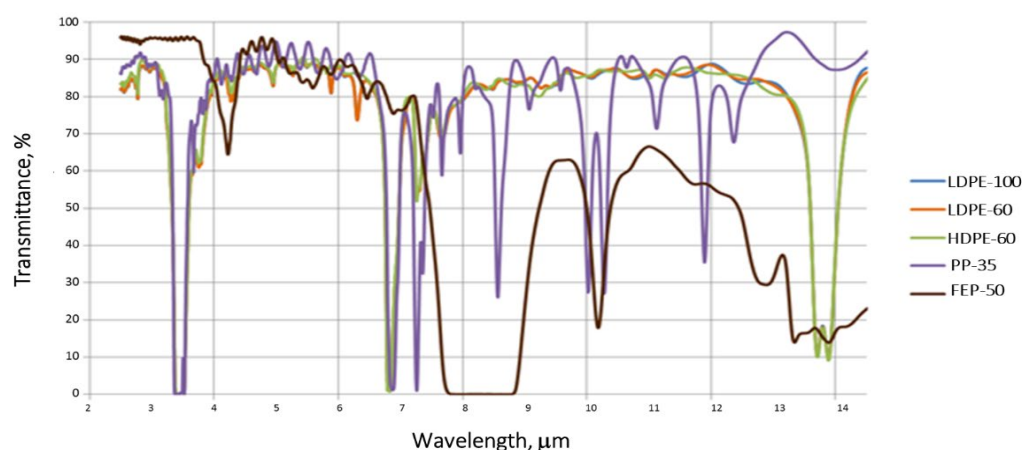


**Figure 7.** FT-IR spectra in the atmospheric window: 0 day samples.

Average transmittances in the atmospheric window (7–14  $\mu\text{m}$ ) were calculated using the weighted average by integration of incoming spectrum [40]. Results for 0 days show transmittances around 79% for the three polyethylene, 75.97% for polypropylene (PP-35) and 37.78% for fluorinated ethylene propylene (FEP-50). These values are in good accordance with the literature [25,26]. Polypropylene shows also high transmittance in the atmospheric window and may be a good candidate for radiative cooling applications (Table 2). However, FEP-50 shows very low transmittance for radiative cooling applications, and it was discarded as a candidate for radiative cooling wind-shields.

**Table 2.** Average transmittances in the atmospheric window.

Average Transmittance, %	LDPE-100	LDPE-60	HDPE-60	PP-35
0 days	79.10	79.17	79.18	75.97
90 days-with glass	76.05	76.27	76.39	74.62
90 days-without glass	76.39	74.03	72.18	73.59

When analyzing Table 2 from an aging perspective, it is seen that average transmittances decrease during 90 days for both polyethylene and polypropylene, as expected and reported by [35]. Transmittance drops may vary depending on the sample cleaning process (manually and maybe not identical for all samples) and the origin of the samples (purchased from different manufacturers). To determine whether this observation is statistically significant, two-tailed *t*-Student tests have been performed (Table 3).

**Table 3.** Comparisons of average transmittances in the atmospheric window.

	Average Transmittance, %			2-Tailed Probability, <i>p</i>		
	0 Days	90 Days with Glass	90 Days without Glass	0 Days/90 Days with Glass	0 Days/90 Days without Glass	90 Days with Glass/90 Days without Glass
LDPE-100	79.10	76.05	76.39	0.999 *	0.999 *	0.435
LDPE-60	79.17	76.27	74.03	0.999 *	1.000 *	0.999 *
HDPE-60	79.18	76.39	72.18	0.999 *	1.000 *	1.000 *
PP-35	75.97	74.62	73.59	0.861	0.992 *	0.754

\* 95%, statistically significant differences.

When comparing the 0 day samples with 90 days for the three polyethylene films, it is seen that after three months of environmental exposure, LDPE and HDPE samples show statistically significant decreases in average transmittance in the atmospheric window. This decrease is observed independently of the thickness and the fact of having the material covered with glass or uncovered. PP-35 shows a significant decrease in transmittance only when the sample was not covered. Last column in Table 3 focuses on samples after 90 days and compares the effect of being covered with glass or uncovered. Both LDPE and HDPE with a thickness of 60  $\mu\text{m}$  show statistical differences, demonstrating the protection role of the glass. Although the aging process exists, samples with glass (higher transmittance values) behave better than those without glass. The protective role of the glass was not observed for LDPE-100, and PP-35, since no statistically significant differences were detected.

FT-IR spectra for each material considering 0 days, 90 days with glass and 90 days without glass are presented (Figures 8–11).

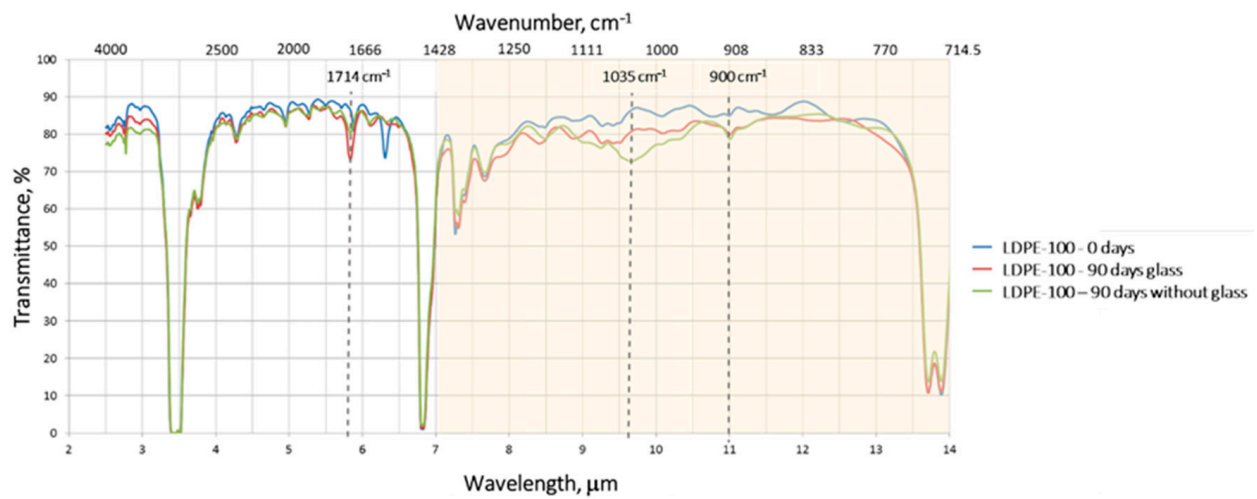


Figure 8. LDPE-100 FT-IR spectra in transmission mode.

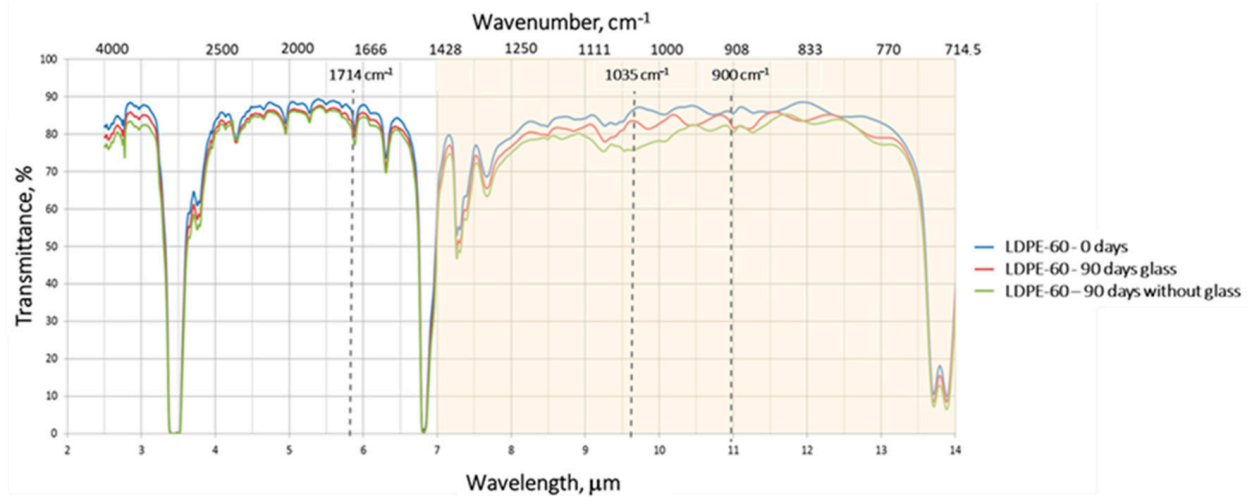


Figure 9. LDPE-60 FT-IR spectra in transmission mode.

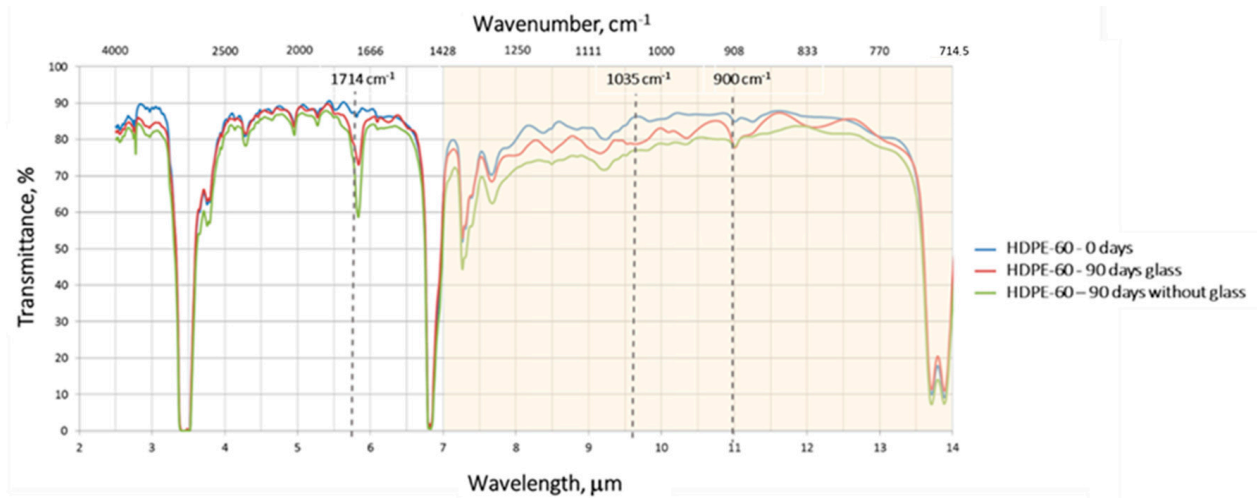
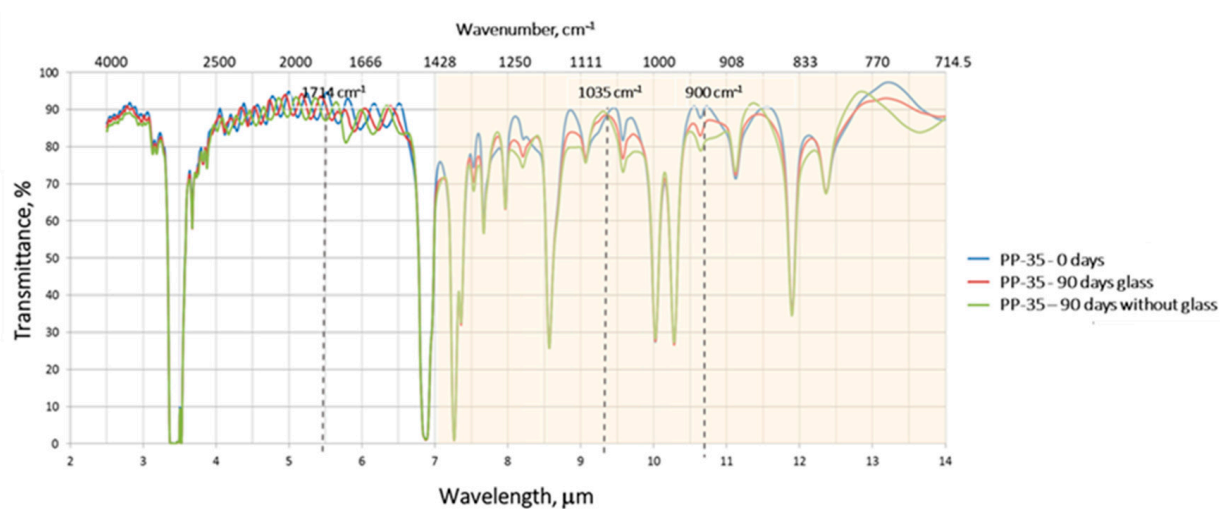


Figure 10. HDPE-60 FT-IR spectra in transmission mode.



**Figure 11.** PP-35 FT-IR spectra in transmission mode.

Spectra for the three polyethylene samples have the same behaviour (Figures 8–10). Higher transmittances are shown for 0 days samples in the atmospheric window and transmittance behaviour is similar for both 90 days samples, with lower transmittances. Spectra for PP-35 are plotted in Figure 11. A common behaviour in the atmospheric window was observed for the three PP-35 samples studied.

Spectra absorption peaks give insight into the degradation of the plastic films. The presence of carbonyl groups, CO bonds and double bonds absorption peaks is presented in Table 4.

**Table 4.** FT-IR spectra qualitative analysis.

		Carbonyl Groups (C=O)	CO Bonds	Double Bonds (C=C)
	Wavenumber, $\text{cm}^{-1}$	1714	1035	900
	Wavelength, $\mu\text{m}$	5.83	9.66	11.11
LDPE-100	0 days	No	No	No
	90 days with glass	Yes	No	Yes
	90 days without glass	Yes	Yes	Yes
LDPE-60	0 days	No	No	No
	90 days with glass	No	No	Yes
	90 days without glass	No	Yes	Yes
HDPE-60	0 days	No	No	No
	90 days with glass	Yes	No	Yes
	90 days without glass	Yes	Yes	Yes
PP-35	0 days	No	No	No
	90 days with glass	No	No	No
	90 days without glass	Yes	No	No

LDPE-100 shows a signal at  $1714 \text{ cm}^{-1}$ , corresponding to the absorption peak of carbonyl groups, which indicates a degradation of polyethylene through an oxidative process. This behaviour was not observed for LDPE-60. For both LDPEs we observed an absorption peak at  $1035 \text{ cm}^{-1}$  in the sample without glass. The  $1035 \text{ cm}^{-1}$  area corresponds to the absorption frequency of CO bonds. Absorption peaks corresponding to double bonds ( $900 \text{ cm}^{-1}$ ) are detected for both LDPE and for 90 days samples with glass and no glass. The three spectra of LDPE-60 show a peak around  $5.8 \mu\text{m}$  but since this peak was already present in the 0 day sample it cannot be attributed to the appearance of carbonyl groups

produced in a degradation process. Thus, no carbonyl groups were detected after 90 days of exposure to the environment.

Figure 10 represents spectra for HDPE-60. The same CO bond absorption frequency area as the one found for LDPE-60 was observed. In addition, narrow peaks at  $1714\text{ cm}^{-1}$  were detected for 90 day samples, meaning that oxidation process existed. Finally, absorption peaks corresponding to double bonds ( $900\text{ cm}^{-1}$ ) are shown in both 90 day samples.

Finally, when analyzing Figure 11 for PP-35 it is seen that curves in the atmospheric window for 0 days and 90 days with glass are very similar and this result matches with the one presented in Table 3, where no significant differences were observed between these two samples. Curves for 0 days and 90 days without glass present slight differences. These differences are statistically significant according to Table 3, meaning that PP-35 suffers some degradation when it is not covered with glass. This is also corroborated by the absorption peak in  $1714\text{ cm}^{-1}$  for 90 days without glass. Unlike what was seen with the other materials, no absorption peaks in the double bond (C=C) absorption band were observed for PP-35.

### 3.2. Mechanical Properties

Young's modulus ( $E_t$ ) and maximum tensile strength ( $\sigma_M$ ) for the four plastic films before exposition and after 90 days covered with glass or without glass are presented in Table 5.

**Table 5.** Young's modulus and maximum tensile strength data for aging study.

Plastic Film	Sample	Glass	$E_t$ (MPa)	$\sigma_M$ (MPa)	Direction *
LDPE-100	0 days		177	22.9	L
	90 days	with	109	10.2	T
	90 days	without	99.7	8.97	L
LDPE-60	0 days		278	24.4	L
	90 days	with	292	19.6	T
	90 days	without	401	20.8	T
HDPE-60	0 days		221	16.8	L
	90 days	with	259	12.3	L
	90 days	without	208	9.2	L
PP-35	0 days		2010	87.9	L
	90 days	with	1810	73.8	L
	90 days	without	4000	200	T

\* where L stands for longitudinal and T for transversal.

The Young's modulus of PP-35 is an order of magnitude larger than the Young's modulus of the PE samples. Knowing that the greater the Young's modulus, the stiffer is the material, PP-35 is stiffer than PE. Maximum tensile strength is about four times larger for PP-35 at the beginning of the experimental campaign and an order of magnitude larger after 90 days. High maximum tensile strength values after 90 days for PP-35 indicate that no scission reactions occurred. Results show that PP-35 can be considered a good wind-shield candidate for radiative cooling.

There was no common pattern when analyzing the effect of the glass in the aging process after 90 days. When looking at Young's modulus it is seen that while LDPE-100 and HDPE-60 show higher values for samples with glass, the opposite behaviour was observed for LDPE-60 and PP-35. The same trend was detected for maximum tensile strength. However, it is worth noticing the different behaviour of PP-35, showing higher differences than polyethylene, between with glass and without glass for both the Young's modulus (120.99%) and maximum tensile strength (171.00%).

Young's modulus and maximum tensile strength before exposition (0 days) tested in the longitudinal and the transversal axis are compared in Table 6. Longitudinal Young's moduli are lower than the transversal ones. Average maximum tensile strength before

degradation for both LDPE-100 and LDPE-60 is 22.7 MPa. This value decreases to 15.85 MPa for HDPE-60 and increases significantly to 117.45 MPa for PP-35.

**Table 6.** Young's modulus and maximum tensile strength data for 0 days samples and for longitudinal and transversal comparison.

Plastic Film	Sample	Direction *	$E_t$ (MPa)		$\sigma_M$ (MPa)	
LDPE-100	0 days	L	177	average	22.9	average
	0 days	T	257	217	22.4	22.70
LDPE-60	0 days	L	278	average	24.4	average
	0 days	T	321	299.50	21.0	22.70
HDPE-60	0 days	L	221	average	16.8	average
	0 days	T	266	243.50	14.9	15.85
PP-35	0 days	L	2010	average	87.9	average
	0 days	T	3370	2690	147	117.45

\* where L stands for longitudinal and T for transversal.

Comparisons between samples without environmental exposure (0 days) and after 90 days of exposure are shown in Table 7. Averages for 0 days longitudinal and transversal samples are calculated. Averages for 90 days samples are also evaluated.

**Table 7.** 0 days and 90 days exposure comparisons: longitudinal and transversal average data for 0 days samples.

Plastic Film	Sample	$E_t$ (MPa)		$\sigma_M$ (MPa)	
LDPE-100	0 days	217.0	variation	22.7	variation
	90 days	104.4	−51.91%	9.6	−57.68%
LDPE-60	0 days	299.5	variation	22.7	variation
	90 days	346.5	+15.69%	20.1	−11.01%
HDPE-60	0 days	243.5	variation	15.9	variation
	90 days	233.5	−4.11%	10.8	−32.18%
PP-35	0 days	2690.0	variation	117.5	variation
	90 days	2905.0	+7.99%	136.9	+16.56%

No common pattern was observed when comparing Young's modulus after 90 days of exposition for each of the four plastic films studied. Average Young's modulus decreases by 51.91% for LDPE-100 while it increases by 15.69% for LDPE-60. The average Young's modulus remains almost constant (decreases 4.11%) for HDPE-60 and increases only 7.99% for PP-35. It is well known that the larger the Young's modulus, the stiffer the sample. According to Meseguer et al. [41] there is a relationship between sample porosity and Young's modulus. When the Young's modulus increases there is a densification effect of the sample and therefore the porosity is lower. Applying this, there is a large increase of sample porosity for LDPE-60.

When analyzing the variation of the maximum tensile strength after 90, we observed a decrement in the three polyethylene samples, being 57.68% for LDPE-100, 11.01% for LDPE-60, and 32.18% for HDPE-60. It is worth noticing the different behaviour of the PP-35, for which an increase of 16.56% was observed. A decrement in the tensile strength demonstrates the presence of scission reactions. According to Chabira et al. [38] chain scissions lead also to a drop of the elongation at break ( $\epsilon_B$ ) and affect adversely the tensile strength. This behaviour is shown in Table 8 where the elongation at break decreases for the three polyethylene samples and increases for PP-35.

**Table 8.** Elongation at break averages for aging study.

Elongation at Break, $\epsilon_B$ (%)	0 Days	90 Days with Glass	90 Days without Glass
LDPE-100	1061.6	903.8	534.1
LDPE-60	760	732.2	716.3
HDPE-60	333.4	122.7	78
PP-35	11.6	NA	21.9

NA stands for not available.

#### 4. Conclusions

This article presents a study of plastic films with thickness between 35–100  $\mu\text{m}$  to determine their suitability to be used as wind-shields for radiative cooling applications. Plastic films samples covered with glass or uncovered and exposed to environmental conditions during 90 days have been studied. FT-IR spectra and traction mechanical tests have been used to study materials degradation.

A decrease in the average transmittance in the atmospheric window between 3.5% and 6.5% for LDPE-100 and LDPE-60, respectively and 9% for HDPE was calculated. PP-35 shows the lowest decrease in transmittance, with a value of 3%.

Polypropylene 35  $\mu\text{m}$  (PP-35) does not show a significant aging process when covered with glass. When the plastic is exposed without glass, the decrease in the average transmittance is only 3%. In addition, FT-IR spectra only show a carbonyl absorption peak for the 90 days samples without glass, confirming a good aging behaviour.

Polypropylene (PP-35) is stiffer than polyethylene (higher Young's modulus and maximum tensile strength). PP-35 after 90 days presents a low increase of Young's modulus (of 7.99%), meaning that there is only a low stiffness of the sample. This result matches with the absence of double bonds and C–O groups in the FT-IR spectra, indicating the good aging behaviour of PP-35. Finally, an increase of 16.56% of the maximum tensile strength for 90 days was observed, indicating that no scission reactions occurred. This explains also while the elongation at break of the PP-35 increases after 90 days.

To sum up, polyethylene has been confirmed as a good candidate to be used as a wind-shield for radiative cooling. Polypropylene has been presented as an alternative because it is also transparent to long-wave radiation but presents better hardness, tensile strength, and elasticity than polyethylene.

**Author Contributions:** Conceptualization, I.M.; methodology, I.M., J.C. and R.V.; formal analysis, I.M. and J.C.; data curation, J.C.; writing—original draft preparation, I.M.; writing—review and editing, J.C., R.V., C.S. and A.C.; supervision, I.M., C.S. and A.C. All authors have read and agreed to the published version of the manuscript.

**Funding:** This publication is part of the grant RTI2018-097669-A-I00, funded by MCIN/AEI/10.13039/501100011033/ and by "ERDF A way of making Europe". This publication is part of the grant PID2021-126643OB-I00, funded by MCIN/AEI/10.13039/501100011033/ and by "ERDF A way of making Europe". The authors would like to thank Generalitat de Catalunya for the project grant given to their research group (2017 SGR 659).

**Data Availability Statement:** Not applicable.

**Conflicts of Interest:** The authors declare no conflict of interest.

#### References

1. Eurostat. Energy Consumption in Households, 2019. Available online: [https://ec.europa.eu/eurostat/statistics-explained/index.php?title=Energy\\_consumption\\_in\\_households#Use\\_of\\_energy\\_products\\_in\\_households\\_by\\_purpose](https://ec.europa.eu/eurostat/statistics-explained/index.php?title=Energy_consumption_in_households#Use_of_energy_products_in_households_by_purpose) (accessed on 30 September 2022).
2. The Future of Cooling. *Opportunities for Energy-Efficient Air-Conditioning*; IEA: Paris, France, 2018.
3. Kasaeian, A.; Bellos, E.; Shamaeizadeh, A.; Tzivanidis, C. Solar-driven polygeneration systems: Recent progress and outlook. *Appl. Energy* **2020**, *264*, 114764. [CrossRef]
4. Vallès, M.; Bourouis, M.; Boer, D. Solar-driven absorption cycle for space heating and cooling. *Appl. Therm. Eng.* **2020**, *168*, 114836. [CrossRef]

5. Bell, E.; Eisner, L.; Young, J.; Oetjen, R. Spectral-Radiance of Sky and Terrain at Wavelengths between 1 and 20 Microns II. *Sky Meas. J. Opt. Soc. Am.* **1960**, *50*, 1313–1320. [[CrossRef](#)]
6. Catalanotti, S.; Cuomo, V.; Piro, G.; Ruggi, D.; Silvestrini, V.; Troise, G. The radiative cooling of selective surfaces. *Sol. Energy* **1975**, *17*, 83–89. [[CrossRef](#)]
7. Granqvist, C.G.; Hjortsberg, A. Radiative cooling to low temperatures: General considerations and application to selectively emitting SiO films. *J. Appl. Phys.* **1981**, *52*, 4205–4220. [[CrossRef](#)]
8. Matsuta, M.; Terada, S.; Ito, H. Solar Heating and radiative cooling using a solar collector-sky radiator with a spectrally selective surface. *Sol. Energy* **1987**, *39*, 83–186. [[CrossRef](#)]
9. Vall, S.; Castell, A.; Medrano, M. Energy Savings Potential of a Novel Radiative Cooling and Solar Thermal Collection Concept in Buildings for Various World Climates. *Energy Technol.* **2018**, *6*, 2200–2209. [[CrossRef](#)]
10. Vall, S.; Medrano, M.; Solé, C.; Castell, A. Combined Radiative Cooling and Solar Thermal Collection: Experimental Proof of Concept. *Energies* **2020**, *13*, 893. [[CrossRef](#)]
11. Hu, M.; Pei, G.; Wang, Q.; Li, J.; Wang, Y.; Ji, J. Field test and preliminary analysis of a combined diurnal solar heating and nocturnal radiative cooling system. *Appl. Energy* **2016**, *179*, 899–908. [[CrossRef](#)]
12. Long, L.; Yang, Y.; Wang, L. Simultaneously enhanced solar absorption and radiative cooling with thin silica micro-grating coatings for silicon solar cells. *Sol. Energy Mater. Sol. Cells* **2019**, *197*, 19–24. [[CrossRef](#)]
13. Ahmed, S.; Li, Z.; Javed, M.S.; Ma, T. A review on the integration of radiative cooling and solar energy harvesting. *Mater. Today Energy* **2021**, *21*, 100776. [[CrossRef](#)]
14. Sakhaei, S.A.; Valipour, M.S. Performance enhancement analysis of the flat plate collectors: A comprehensive review. *Renew. Sustain. Energy Rev.* **2019**, *102*, 186–204. [[CrossRef](#)]
15. Hu, M.; Zhao, B.; Ao, X.; Su, Y.; Pei, G. Numerical study and experimental validation of a combined diurnal solar heating and nocturnal radiative cooling collector. *Appl. Therm. Eng.* **2018**, *145*, 1–13. [[CrossRef](#)]
16. Chen, Z.; Zhu, L.; Li, W.; Fan, S. Simultaneously and Synergistically Harvest Energy from the Sun and Outer Space. *Joule* **2019**, *3*, 101–110. [[CrossRef](#)]
17. Hu, M.; Suhendri; Zhao, B.; Ao, X.; Cao, J.; Wang, Q.; Riffat, S.; Su, Y.; Pei, G. Effect of the spectrally selective features of the cover and emitter combination on radiative cooling performance. *Energy Built Environ.* **2021**, *2*, 251–259. [[CrossRef](#)]
18. Vilà, R.; Martorell, I.; Medrano, M.; Castell, A. Adaptive covers for combined radiative cooling and solar heating. A review of existing technology and materials. *Sol. Energy Mater. Sol. Cells* **2021**, *230*, 111275. [[CrossRef](#)]
19. Zhang, J.; Yuan, J.; Liu, J.; Zhou, Z.; Sui, J.; Xing, J. Cover shields for sub-ambient radiative cooling: A literature review. *Renew. Sustain. Energy Rev.* **2021**, *143*, 110959. [[CrossRef](#)]
20. Bosi, S.G.; Bathgate, S.N.; Mills, D.R. At Last! A Durable Convection Cover for Atmospheric Window Radiative Cooling Applications. *Energy Procedia* **2014**, *57*, 1997–2004. [[CrossRef](#)]
21. Chen, Z.; Zhu, L.; Raman, A.; Fan, S. Radiative cooling to deep sub-freezing temperatures through a 24-h day–night cycle. *Nat. Commun.* **2016**, *7*, 13729. [[CrossRef](#)]
22. Laatioui, S.; Benlattar, M.; Mazroui, M.; Saadouni, K. Zinc monochalcogenide thin films ZnX (X = S, Se, Te) as radiative cooling materials. *Optik* **2018**, *166*, 24–30. [[CrossRef](#)]
23. Hjortsberg, A.; Granqvist, C.G. Radiative cooling with selectively emitting ethylene gas. *Appl. Phys. Lett.* **1981**, *39*, 507–509. [[CrossRef](#)]
24. Xu, G.; Zhang, L.; Wang, B.; Chen, X.; Dou, S.; Pan, M.; Ren, F.; Li, X.; Li, Y. A visible-to-infrared broadband flexible electrochromic device based polyaniline for simultaneously variable optical and thermal management. *Sol. Energy Mater. Sol. Cells* **2020**, *208*, 110356. [[CrossRef](#)]
25. Hu, M.; Pei, G.; Li, L.; Zheng, R.; Li, J.; Ji, J. Theoretical and Experimental Study of Spectral Selectivity Surface for Both Solar Heating and Radiative Cooling. *Int. J. Photoenergy* **2015**, *2015*, 807875. [[CrossRef](#)]
26. Carrobé, A.; Martorell, I.; Solé, C.; Castell, A. Transmittance analysis for materials suitable as radiative cooling windshield and aging study for polyethylene. In Proceedings of the Eurosun 2020 Conference, Athenes, Greece, 1–4 September 2020.
27. Abdelhafidi, A.; Babaghayou, I.M.; Chabira, S.F.; Sebaa, M. Impact of Solar Radiation Effects on the Physicochemical Properties of Polyethylene (PE) Plastic Film. *Procedia-Soc. Behav. Sci.* **2015**, *195*, 2922–2929. [[CrossRef](#)]
28. Balocco, C.; Mercatelli, L.; Azzali, N.; Meucci, M.; Grazzini, G. Experimental transmittance of polyethylene films in the solar and infrared wavelengths. *Sol. Energy* **2018**, *165*, 199–205. [[CrossRef](#)]
29. Albertsson, A.-C.; Andersson, S.O.; Karlsson, S. The mechanism of biodegradation of polyethylene. *Polym. Degrad. Stab.* **1987**, *18*, 73–87. [[CrossRef](#)]
30. Carrasco, F.; Pagès, P.; Pascual, S.; Colom, X. Artificial aging of high-density polyethylene by ultraviolet irradiation. *Eur. Polym. J.* **2001**, *37*, 1457–1464. [[CrossRef](#)]
31. Almond, J.; Sugumaar, P.; Wenzel, M.N.; Hill, G.; Wallis, C. Determination of the carbonyl index of polyethylene and polypropylene using specified area under band methodology with ATR-FTIR spectroscopy. *e-Polymers* **2020**, *20*, 369–381. [[CrossRef](#)]
32. Chabira, S.; Mohamed, S.; Hadj Aissa, B. The Use of Mechanical Testing in the Study of Plastic Films Degradation. *Rev. Des Sci. Et Sci. L'ingénieur* **2013**, *3*, 28–32.
33. Rouillon, C.; Bussiere, P.-O.; Desnoux, E.; Collin, S.; Vial, C.; Therias, S.; Gardette, J.-L. Is carbonyl index a quantitative probe to monitor polypropylene photodegradation? *Polym. Degrad. Stab.* **2016**, *128*, 200–208. [[CrossRef](#)]

34. Zhao, B.; Zhang, S.; Sun, C.; Guo, J.; Yu, Y.X.; Xu, T. Aging behaviour and properties evaluation of high-density polyethylene (HDPE) in heating-oxygen environment. *IOP Conf. Ser. Mater. Sci. Eng.* **2018**, *369*, 012021. [[CrossRef](#)]
35. Ali, A.H.H.; Saito, H.; Taha, I.M.S.; Kishinami, K.; Ismail, I.M. Effect of aging, thickness and color on both the radiative properties of polyethylene films and performance of the nocturnal cooling unit. *Energy Convers. Manag.* **1998**, *39*, 87–93. [[CrossRef](#)]
36. Martorell, I.; Camarasa, J.; Vilà, R.; Solé, C.; Castell, A. RCE as a device to produce heating and cooling. Transmittance and aging study for cover materials suitable for radiative cooling. In Proceedings of the ICP 2021, Virtual, 22–25 September 2021.
37. Sebaa, M.; Servens, C.; Pouyet, J. Natural and artificial weathering of low-density polyethylene (LDPE): Calorimetric analysis. *J. Appl. Polym. Sci.* **1992**, *45*, 1049–1053. [[CrossRef](#)]
38. Chabira, S.F.; Huchon, R.; Sebaa, M. Anisotropic character and ultrasonic stiffness changes during the natural weathering of LDPE films. *J. Appl. Polym. Sci.* **2003**, *90*, 559–564. [[CrossRef](#)]
39. Chabira, S.F.; Sebaa, M.; Huchon, R.; De Jeso, B. The changing anisotropy character of weathered low-density polyethylene films recognized by quasi-static and ultrasonic mechanical testing. *Polym. Degrad. Stab.* **2006**, *91*, 1887–1895. [[CrossRef](#)]
40. Bergman, T.L.; Incropera, F.P.; DeWitt, D.P.; Lavine, A.S. *Fundamentals of Heat and Mass Transfer*, 7th ed.; John Wiley & Sons: Hoboken, NJ, USA, 2011; ISBN 978-0470-50197-9.
41. Meseguer-Dueñas, J.M.; Más-Estellés, J.; Castilla-Cortázar, I.; Escobar Ivirico, J.L.; Vidaurre, A. Alkaline degradation study of linear and network poly( $\epsilon$ -caprolactone). *J. Mater. Sci. Mater. Med.* **2011**, *22*, 11–18. [[CrossRef](#)]